RESISTANCE OF AL-BASED COATING IN LIQUID METAL ENVIRONMENT OF 625 STEEL

[1]Lucia ROZUMOVÁ, [1]Martina PAZDEROVÁ, [2]Lukáš KOŠEK

[1]Centrum výzkumu Řež s.r.o., Hlavní 130, Řež, 250 68 Husinec, Czech Republic, EU
[2]VŠCHT Praha, Prague, Dejvice, Czech Republic, EU
lucia.rozumova@cvrez.cz

https://doi.org/10.37904/metal.2024.4948

Abstract

The corrosion resistance of the aluminum-based coating deposited on Inconel Alloy 625 by CVD method was investigated. Specimens of 625 Alloy in as-received state and coated were exposed to static liquid lead at 520 °C. The aim of work was to compare and evaluate the resistance of the coating in different conditions. Two expositions were studied - low oxygen content 10^{-8} wt.% for 3500 h and cycling of temperature for 1000 h. The results indicate that coatings have good adhesion and could protect the studied alloy from lead corrosion. However, several microscopic anomalies the so-called inner oxidation of alloy under the coating were observed. Corrosion damage was characterized using scanning electron microscopy, which identified the inner oxidation under the coating after exposition. Coating was intact, uniformly applied, without cracks. Local depletion of Cr and Ni was observed within 4.1 μm for low oxygen content and 4.5 μm for cycling exposure and solution-based attack (SBA) was not observed. Specimens without coating were very damaged and destroyed in both exposures because deep penetration of lead was observed.

Keywords: 625 steel, liquid lead, corrosion, coating

1. INTRODUCTION

Superalloys, renowned for their exceptional tensile strength, high-temperature yield strength, resistance to creep, and corrosion resistance, find extensive utilization in advanced engineering applications. These superalloys have mainly been developed to high temperature environment. These alloys have a high strength/weight ratio and high-temperature corrosion and erosion resistance compared to conventional alloys [1, 2, 3, 4]. Inconel 625 is a nickel-based superalloy with an exceptional resistance to oxidation, local types of corrosion (inter-crystalline, crevice, pitting, corrosion cracking, etc.) and excellent combination of strength and plasticity both at negative and high temperatures reaching 900 - 1200 °C due to its notable alloying additions such as Nb, Cr, Mo, and Fe [5, 6]. Inconel 625 is used for various applications such as nuclear, aerospace, chemical and petrochemical industries, gas turbine engines etc. [7].

Liquid lead-bismuth eutectic (LBE), Pb-Li alloys and liquid Pb are the proposed coolants for the future high temperature nuclear applications, like nuclear reactor, fusion, and solar powered devices. Therefore, understanding the interaction of the liquid lead with the proposed structural materials at high temperatures is necessary. Most of the liquid lead corrosion studies are reported on bare steels or steels with different types of coatings. However, the study of liquid lead corrosion behavior of aluminized Ni-base alloys is not yet reported.

The application of protective and suitable coating is one of the mitigation methods to overcome materials degradation under elevated temperature conditions. Aluminide based coatings are found to be very effective to improve the oxidation behavior of the alloy at high temperatures [8, 9, 10, 11]. In this respect, Al_2O_3 coatings are considered as an ideal candidate, owing to the beneficial combination of good chemical inertness and hardness at high temperature [12, 13]. Chemical Vapor Deposition (CVD) is a method for producing low stress

coatings by means of thermally induced chemical reactions. The most significant advantage of CVD coating is a uniform and conformal coverage of the surface. However, the main drawback of these CVD coatings is the evolution of residual tensile stresses during the cooling from a deposition temperature of about 1000 °C to room temperature, which limits the use of materials such as austenitic steel 316L or ferritic/martensitic steel T91 [14].

In the present study, Al-based coating was deposited on Inconel 625 alloy using CVD method. The coated alloy was exposed in liquid metal and characterized using SEM, EDS and measured data were statistically evaluated.

2. EXPERIMENTAL MATERIAL

2.1. Base material

The chemical composition of the Inconel 625 superalloy used for this study is presented in **Table 1**. The Inconel 625 alloy was produced by melting and rolling to a thickness of 1.5 mm (VDM Metals GmbH, melt 24773-0232, ASTM B443). After the rolling, a normalization heat-treatment at 950 °C for 30 min and cooling in water were carried out by the manufacturer.

Table 1 Nominal composition of Inconel 625 (wt. %).

Alloy	Al	Cr	Co	Fe	Ni	Mo	Nb+Ta	Ti	Si	C	Mn	S	Ta	P	Cu
Inconel625	0.25	22.27	0.04	4.57	59.58	9.19	3.43	0.33	0.13	0.03	0.10	0.001	<0.01	0.007	0.02

2.2. Coating

CVD method was used to produce an Al-based coating. Specimens of In625 alloy used for experiments were prepared with TiN/TiCN/kappa-Al_2O_3 coating by Bernex 29 HSE (IHI Ionbond AG). The coating architecture consists of multiple layers grown on surface of the specimen in the following order: a base layer TiN (diffusion barrier) followed by top layer, made of kappa-Al_2O_3, respectively.

2.3. Samples

Corrosion coupons were used for the experiments. The dimensions of the tested specimens were 20 x 5 x 1.5 mm (Figure 1). Before exposure, all specimens were ultrasonically cleaned with acetone and dried.

Figure 1 Sample of Inconel 625 alloy in the holder before exposure

2.4. Corrosion experiments in liquid lead

An instrumented static tank was used for experiments with liquid lead, see (**Figure 2**). Static tank consists of a 4.5 l stainless-steel test chamber lined with alumina (Al_2O_3) crucible which prevents the direct contact of the steel walls with the Pb during the exposure. The melting of the lead is done using heating elements which are reeled onto the chamber outer surface allow controlling the test temperature. The thermal insulation of the whole setup minimizes potential heat losses and high temperature ensures gradient in the liquid lead bath. The static tank has the air-lock and the test chamber which separates from each other a ball valve. The air-lock chamber is used for vacuuming of the specimens in an inert gas atmosphere both before and after their immersion into the liquid metal to avoid oxidation during heating up and cooling down. A simple immersion method was used for testing at static conditions. First, the specimens in holder were vacuumed by pure argon, lead was heated up to 520 °C to melt. After the melt stabilization, the holders with the fixed test specimens were immersed from the air-tight air-lock chamber into the liquid lead. The automatic gas mixing was used to ensure the required oxygen concentration values ($Ar+H_2$ (6 %) with $Ar+O_2$ (10 %)). Active oxygen control, i.e., maintaining the oxygen concentration in the Pb at the targeted level, was based on the oxygen sensor signal measurement. A reducing $Ar+H_2$ (6 %) gas mixture was used as a cover gas. Oxygen sensors based on the Bi/Bi_2O_3 ref. electrode were used.

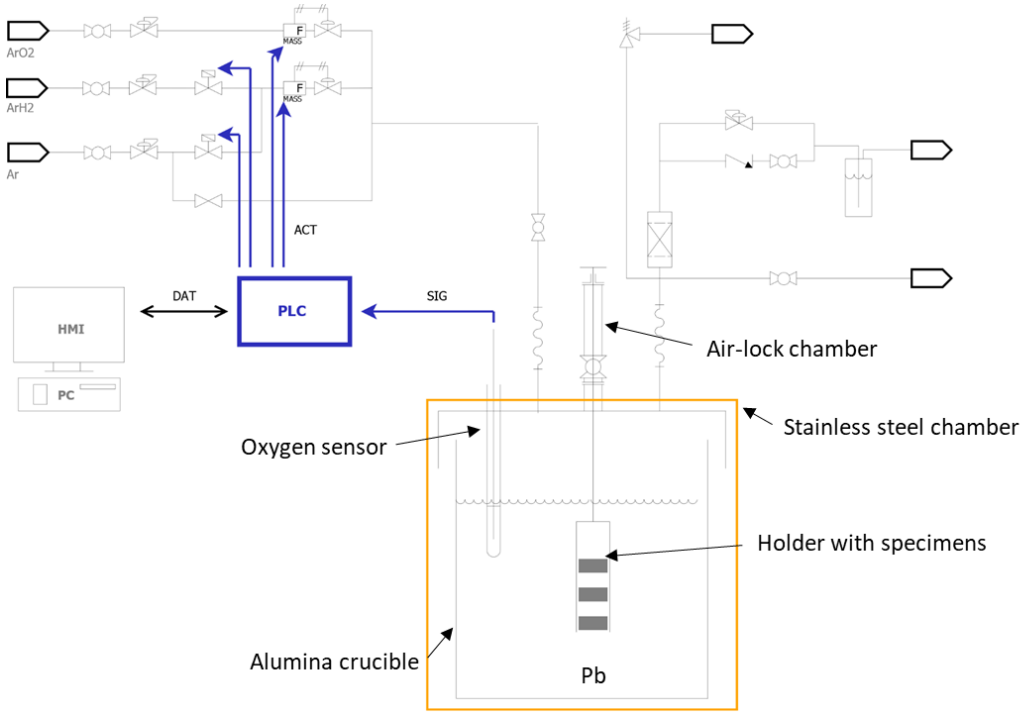

Figure 2 Scheme of experimental setup

The prepared specimens were used for two exposures. The first experiment was made with low oxygen concentration 10^{-8} wt. % in lead with a target temperature of 520 °C for 3500 h. The second experiment was made with high oxygen concentration 10^{-6} wt. % in lead for 1000 h. The temperature cycling was performed in this experiment, 168 h for 520 °C about 5 hours transition to temperature 450 °C for next 168 h with a total exposure time of 1000 h.

After exposure, the specimens were metallographically cut, metallographically ground using sandpaper and polished using a diamond paste. This process was followed by the analysis and thickness measurements of the oxide layer and for specimens with a coating, the resistance of the coating was evaluated from the point of view of the protection of the base material. The evaluation of the surface layers was carried out using a

Scanning Electron Microscope (SEM, LYRA3 and MIRA 3 TESCAN) equipped with detectors for the imaging of Backscatter Electrons (BSE) and Energy Dispersive Spectroscopy (EDS) for chemical analysis.

3. RESULTS AND DISCUSSION

3.2. Low oxygen experiment with stable conditions of temperature

Post test observation by SEM showed very deep solution-based attack (SBA) including lead penetration into the base material. The SBA part reached a maximum deep of 75 µm and total affected area reached 100 % from the entire perimeter of the monitored sample. The cross-sections evaluation did not reveal the presence of the protective passive layer. The corrosion mechanism of the sample can be defined as a layer enrichment towards the surface by Cr and at the same time the depletion of this part by Ni and at the same time lead penetration into the base material.

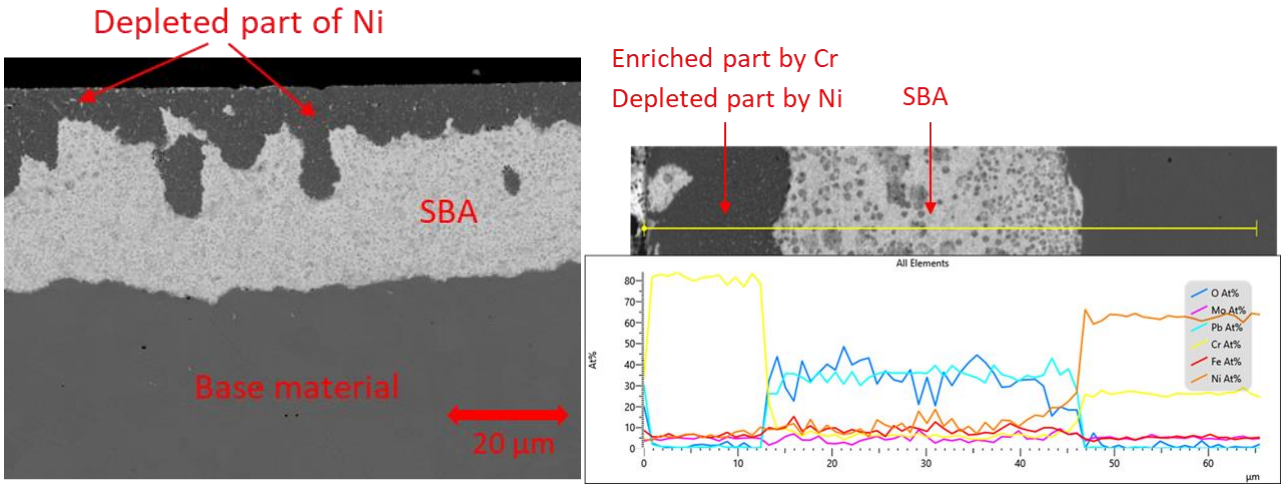

Figure 3 SEM image and EDX line pattern after 3500 h exposure of In625 without coating

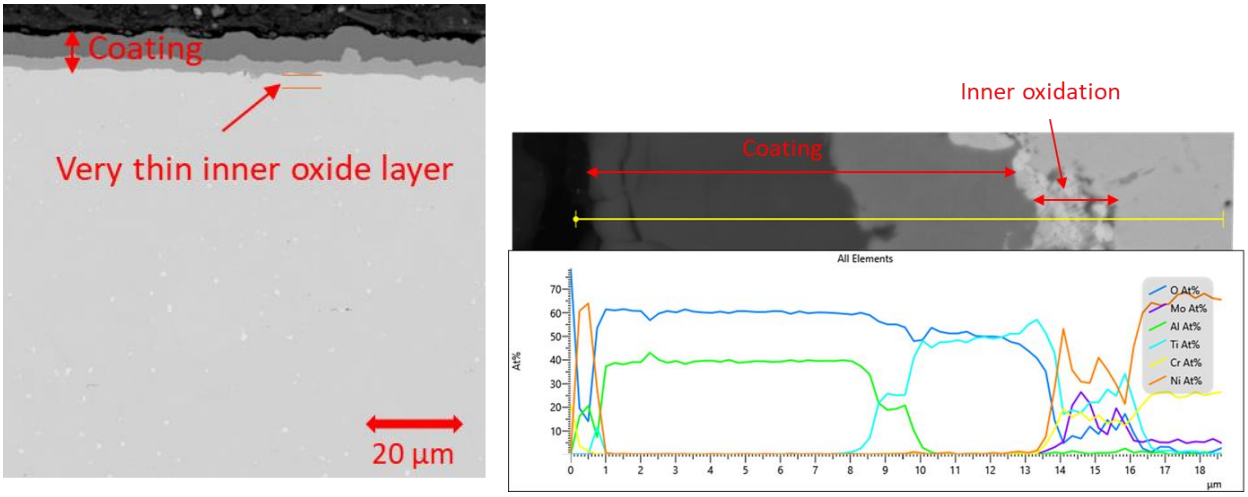

Figure 4 SEM image and EDX line pattern after 3500 h exposure of In625 with Al_2O_3 coating

The evaluation of the coating after exposure showed that the coating has a stable, uniform, and compact structure without defects. The coating had uniform thickness around 10 µm, composed of an outer layer of

aluminum oxide and an inner layer of titanium oxide. The inner layer of the coating was enriched by oxide. Formation of a thin inner oxide layer under the coating was observed (**Figure 4**). Lead penetration to the base material and coating was not observed. The EDX analysis data across the coating/oxide/alloy interfaces is presented in (**Figure 4**) (EDX line pattern). The thin inner layer under the coating containing oxide and enriched with Mo and Ti, at the same time, this layer is depleted by Cr and Ni. The total area affected by inner oxidation reached approximately 12% of the surface and the maximum depth of the inner oxidation reached 4.1 µm.

3.3. High oxygen experiment with cycling of temperature

SEM analysis of specimen cross-section showed that combination of high oxygen content and cycling of temperature was for In625 alloy crucial. As can be seen in (**Figure 5**), SBA and penetration of lead into the alloy is significant. The total affected area reached 97% and the maximum depth was more than 1000 µm. SBA part was enriched by Cr and depleted by Ni.

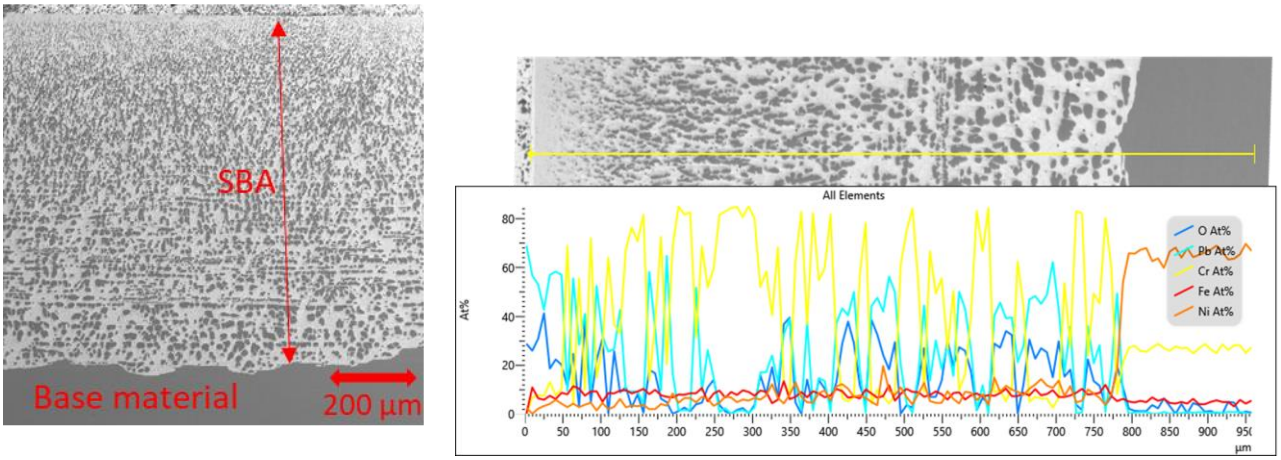

Figure 5 SEM image and EDX line pattern after 1000 h exposure of In625 without coating

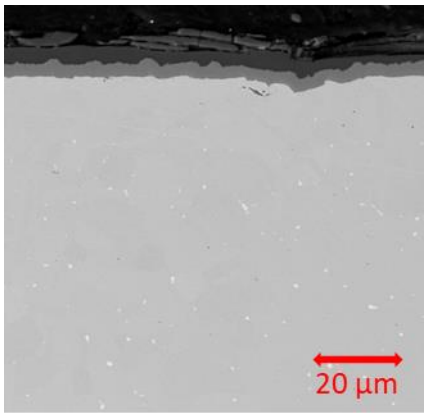

Figure 6 SEM image after 1000 h exposure of In625 with Al_2O_3 coating

SEM analysis showed that the coating has the same uniform and stable structure like in the first experiment (Figure 6). The coating performed a protective function compared to the result without the coating (**Figure 5**). The coating was composed from an outer (Al-based) and an inner layer (Ti-based). Formation of a thin inner oxide layer under the coating was observed. The total area affected by inner oxidation reached approximately 54 % of the surface and the maximum depth of the inner oxidation reached 4.5 µm.

4. CONCLUSION

In this paper corrosion resistance of In625 with and without coating was evaluated. The specimens were exposed to liquid lead with two different conditions – low oxygen content for 3500 h and high oxygen content with cycling of temperature. In conclusion, it can be said that:

- specimens without coating suffered from SBA and penetration of lead into the base material, 97-100 % of the observed surface was attacked,
- the coating showed a high resistance to both exposures, specimens with coating were without SBA and penetration of lead, only a thin layer of inner oxide was found.

ACKNOWLEDGEMENTS

This research was funded by the Technology Agency of the Czech Republic (TACR), grant number TK04030082, and the presented results were obtained using the CICRR infrastructure, which was funded by the Ministry of Education, Youth and Sports, grant number LM2023041.

REFERENCES

[1] DONACHIE, M.J., DONACHIE, S.J. *Superalloys: A Technical Guide*. ASM International, 2002.

[2] REED, R.C. *The Superalloys: Fundamentals and Applications*. Cambridge University Press, 2008.

[3] GRABOŚ A., RUTKOWSKI P., HUEBNER J., KOZIEŃ D., ZHANG S., KUO Y.L., HAYASHI S. Oxidation Performance of Spark Plasma Sintered Inconel 625-NbC Metal Matrix Composites. *Corrosion Science*, 2022, vol. 205, 110453.

[4] DUDZIAK T., BORON L., GUPTA A., SARAF S., SKIERSKI P., SEAL S. Steam Oxidation Resistance and Performance of Newly Developed Coatings for Haynes® 282® Ni-based Alloy. *Corrosion Science*, 2018, vol. 138, pp. 326-339.

[5] Hu Y., Lin X., Li Y., Ou Y., Gao X., Zhang Q., Li W., Huang W. Strengthening Mechanisms in Polycrystalline Nickel-based Superalloys. *Materials Science and Technology*, 2021, vol. 34 (15), pp. 1793-1808.

[6] DHARMENDRA C., HADADZADEH A., AMIRKHIZ B.S., JANAKI RAM G.D., MOHAMMADI M. Microstructural evolution and mechanical behavior of nickel aluminum bronze Cu-9Al-4Fe-4Ni-1Mn fabricated through wire-arc additive manufacturing. *Additive Manufacturing*, 2019, vol. 30, 100872.

[7] MAJUMDAR S., BORGOHAIN A., KAIN V. Interaction between liquid lead-bismuth eutectic and aluminized Inconel 625 superalloy at 600 and 850 °C. *Journal of Nuclear Materials*, 2019, 518, pp. 54-61.

[8] GOWARD G.W., BOONE D.H. Mechanisms of formation of diffusion aluminide coatings on nickel-base superalloys. *Oxidation of Metals*, 1971, 3, pp. 475-494.

[9] PAULETTI E., D'OLIVEIRA A.S.C.M. Influence of Pt concentration on structure of aluminized coatings on a Ni base superalloy. *Surface and Coatings Technology*, 2017, 332, pp. 57-63.

[10] CAO G.H., YAO P.P., FU C., RUSSELL A.M. Microstructure and oxidation behavior of Al and Hf co-deposition coatings on nickel-based superalloys. *Surface and Coatings Technology*, 2013, 224, pp. 57-61.

[11] TAWANCY H.M. On the microstructures of platinum aluminide bond coatings produced by different aluminizing methods: effects on the performance of thermal barrier coatings on Ni-based superalloys. *Metallography, Microstructure, and Analysis*, 2018, 7, pp. 363-369.

[12] FALLQVIST M., RUPPI S., OLSSON M., OTTOSSON M., GREHK T.M. Nucleation and growth of CVD α-Al2O3 on TixOy template. *Surface & Coatings Technology*, 2012, 207, pp. 254-261.

[13] STYLIANOU R., TKADLETZ M., SCHALK N., PENOY M., CZETTL C., MITTERER C. Effects of reference materials on texture coefficients determined for a CVD α-Al2O3 coating. *Surface & Coatings Technology*, 2019, 359, pp. 314-322.

[14] SCHODERBÖCK P. Chemical vapor deposited alumina hard coatings: residual stress states decisively determined by the physical material properties. Materialia, 2022, 21.